RELATIVISTIC COULOMB EXCITATION OF ^{124}Sn*

I. Lihtar[a], E. Kudaibergenova[b], M. Feijoo-Fontán[c], I. Gašparić[a]
A. Horvat[a,b], T. Aumann[b,d,e], D. Rossi[b,d], V. Panin[d]
J.L. Rodriguez-Sanchez[c,f], H. Alvarez-Pol[c], L. Atar[b], J. Benlliure[c]
C.A. Bertulani[g], K. Boretzky[d], L.T. Bott[h], C. Caesar[d], E. Casarejos[i]
J. Cederkall[j], A. Chatillon[k], D. Cortina-Gil[c], E. De Filippo[l]
T. Dickel[d], M. Duer[b], A. Falduto[b], D. Galaviz[m], G. García-Jiménez[c]
Z. Ge[d], E.I. Geraci[n], R. Gernhäuser[o], B. Gnoffo[n]
A. Graña-González[c], K. Göbel[h], E. Haettner[d], A.L. Hartig[b], M. Heil[d]
A. Heinz[p], T. Hensel[q], M. Holl[p], A. Jedele[b], D. Jelavić Malenica[a]
T. Jenegger[o], L. Ji[b], H.T. Johansson[p], B. Jonson[p]
N. Kalantar-Nayestanaki[r], A. Kelić-Heil[d], O.A. Kiselev[d], P. Klenze[b]
D. Körper[d], T. Kröll[b], Yu.A. Litvinov[d], B. Löher[d], N.S. Martorana[s]
L.M. Fonseca[b], P. Morfouace[k], S. Murillo-Morales[t], C. Nociforo[d]
A. Obertelli[b], S. Paschalis[s], A. Perea[u], M. Petri[t], S.B. Pietri[d]
S. Pirrone[l], L. Ponnath[o], H.B. Rhee[d], L. Rose[t], P. Russotto[s]
D. Savran[d], H. Scheit[d], H. Simon[d], J.P. Simon[d], S. Storck-Dutine[b]
A. Stott[t], Y. Sun[d], D. Symochko[d], C. Sürder[d], J. Taieb[k], R. Taniuchi[t]
O. Tengblad[u], H.T. Törnqvist[b,p], S. Velardita[b], F. Wamers[d]
and the R3B Collaboration

[a]Ruđer Bošković Institute, Bijenička cesta 54, 10000, Zagreb, Croatia
[b]Technische Universität Darmstadt, Fachbereich Physik, Institut für Kernphysik 64289 Darmstadt, Germany
[c]IGFAE, Universidade de Santiago de Compostela, 15782 Santiago de Compostela, Spain
[d]GSI Helmholtzzentrum für Schwerionenforschung, Planckstraße 1, 64291, Darmstadt, Germany
[e]Helmholtz Research Academy Hesse for FAIR, 64289 Darmstadt, Germany
[f]CITENI, Campus Industrial de Ferrol, Universidade da Coruña, 15403, Ferrol, Spain
[g]Texas A&M University-Commerce, 75428, Commerce, TX, USA
[h]Goethe-Universität Frankfurt, Max-von-Laue Str. 1, 60438, Frankfurt am Main, Germany
[i]CINTECX, Universidade de Vigo, DSN, Dpt. Mech. Engineering, 36310 Vigo, Spain
[j]Lund University, Department of Physics, P.O. Box 118, 221 00, Lund, Sweden
[k]CEA, DAM, DIF, 91297 Arpajon Cedex, France
[l]INFN Sezione di Catania, Via Santa Sofia 64, 95123, Catania, Italy
[m]LIP-Lisbon, 1649-016 Lisboa, Portugal
[n]Università di Catania, Dipartimento di Fisica e Astronomia "Ettore Majorana", Catania, Italy
[o]Technische Universität München, James-Franck-Str. 1, 85748, Garching, Germany
[p]Institutionen för Fysik, Chalmers Tekniska Högskola, 412 96 Göteborg, Sweden
[q]Helmholtz-Zentrum Dresden-Rossendorf, Institute of Radiation Physics Bautzner Landstraße 400, 01328, Dresden, Germany
[r]ESRIG, University of Groningen, Groningen, The Netherlands
[s]INFN Laboratori Nazionali del Sud, Via Santa Sofia 62, 95123, Catania, Italy
[t]School of Physics, Engineering and Technology, University of York, YO10 5DD York, UK
[u]Instituto de Estructura de la Materia, CSIC, 28006 Madrid, Spain

Received 10 November 2023, accepted 4 January 2024, published online 24 April 2024

* Presented at the XXXVII Mazurian Lakes Conference on Physics, Piaski, Poland, 3–9 September, 2023.

The Coulomb excitation of ^{124,128,130,132,134}Sn isotopes in the electric field of a Pb target have been studied using the R^{3}B setup as a part of the FAIR Phase-0 program. The experiment was motivated by the possibility of using the nuclear dipole response to infer valuable information on the slope of the symmetry energy of the nuclear equation of state. Measurements were performed in inverse kinematics at relativistic energies of 750 MeV/u and 904 MeV/u. The analysis method and preliminary results for the decay channel with a single outgoing neutron for ^{124}Sn are reported.

DOI:10.5506/APhysPolBSupp.17.3-A17

1. Introduction

The electromagnetic interaction can be a resourceful tool to probe the underlying details of nuclear structure and dynamics [1]. One such case is the relativistic Coulomb excitation of heavy nuclei. When a heavy nucleus moving at highly relativistic speeds (in our case $\beta > 0.8$) gets exposed to a Coulomb field of a high-Z target, collective excitations, mostly of electric dipole (E1) character, are initiated. The E1 response of heavy neutron-rich nuclei is comprised of two main components — the giant dipole resonance (GDR) at higher excitation energies and the pygmy dipole resonance (PDR) at lower ones (see *e.g.* [2]). The GDR exhausts a major part of the dipole strength and can be viewed as an out-of-phase oscillation between the proton and neutron densities of the nucleus. At lower energies, a fraction of the dipole strength forms the so-called PDR, which can be macroscopically interpreted as an oscillation of the neutron skin around the isospin symmetric core. Hence, the nuclear dipole response reflects the isospin imbalance of the system. This can be utilized to place a constraint on the slope of the symmetry energy L of the nuclear equation of state (EOS) — a task that requires an isospin-sensitive observable. Major research efforts are nowadays addressing this topic since a better understanding of the nuclear symmetry energy would help yield answers to open questions in both nuclear structure and astrophysics [3].

The Coulomb excitation cross section (σ_{C}) at high beam energies is a quantity that contains the information about the E1 response of the nucleus. It can be studied by measuring neutron and gamma decay after excitation. Experimentally, it is more easily accessible than the full excitation spectrum of the nucleus and for the purpose of constraining L, it carries essentially the same information as the dipole polarizability [4], a well-established observable in EOS studies [5]. This work aims to extract σ_{C} above the one-neutron separation threshold for the available tin isotopes in the mass range of 124–134.

2. Experiment

The experiment was performed at the GSI Helmholtz Centre for Heavy Ion Research. The UNILAC, SIS18, and FRS facilities were used for the acceleration of the primary beam, production of the secondary beam, and transport of the latter to the R^{3}B (Reactions with Relativistic Radioactive Beams) experimental setup. Production of the secondary cocktail beam centered around ^{124}Sn was ensured through fragmentation of ^{136}Xe on a Be target while for the production of the neutron-rich Sn isotopes in the mass range of 128–134, fission of ^{238}U on a Pb production target was used.

Incoming beam identification (ID) is achieved with the $B\rho$–ΔE-ToF method [6]. On this account, the value for the magnetic rigidity $B\rho$ is determined by using $B\rho_0$ of the centered ion (known from magnet settings) and the lateral deviation from the centered ion trajectory measured at the $S2$ focal plane of the FRS. The charge is obtained from the energy deposited in a thin segmented silicon detector, while the time of flight is measured between scintillators at the $S2$ focal plane of the FRS and the start detector at the entrance of the R^{3}B setup. After passing through incoming identification detectors, the beam impinged on different secondary targets. Carbon (1 g/cm^2), lead (0.98 g/cm^2), and an empty target frame were used for measuring σ_{C}.

The target area was surrounded by the γ-ray detector CALIFA [7] comprised of CsI(Tl) crystals covering angles in the range of 19°–90°. Closely downstream an ionization chamber was installed for accurate fragment charge determination followed by a multi-wire proportional chamber for measurement of the x and y positions. Charged fragments were then bent in the superconducting GLAD magnet in order to separate them according to their mass-over-charge ratio A/Q, and detected in several tracking detectors along the fragment arm. Scintillator fiber detectors were placed to measure the x and y positions of the fragments at several locations along the fragment trajectory, while a scintillator wall [8] was used at the end of the path for final charge and time-of-flight (with respect to the start detector) measurement. Information from the tracking detectors is used in a multidimensional fit routine determining fragment mass with 0.2% (sigma) resolution. Evaporated neutrons from the fragment followed straight trajectories, about 16 m long, from the reaction point to the NeuLAND neutron detector [9] where their time of flight and position were measured.

Measurement of σ_{C} is attainable with this arrangement in inverse kinematics (which is used since most of the studied isotopes are short-lived) and high relativistic energies such that reaction products are Lorentz boosted in the laboratory frame of reference ensuring high acceptance. The lead target is used because of its high Coulomb field. Considering possible nuclear reactions, mostly knockout channel will be populated. With this setup, one

also benefits from the nature of the angular distribution of knocked out nucleons. Their distribution peaks at 45° [10] and since the neutron detector covers roughly up to 7° in scattering angle, only the tail of this distribution will be in the acceptance, making neutrons from de-excitation of dipole resonances the majority. The contribution from inelastic nuclear scattering is subtracted using measurements on the carbon target.

3. Results and discussion

The ^{124}Sn setting at 904 MeV/u has been analyzed and a preliminary one-neutron decay channel σ_{C} was obtained from the data. Other isotopes as well as higher multiplicities of neutrons will be the focus of further investigations. For the determination of a one-neutron cross section, proper particles in the incoming and outgoing channel need to be selected. In the incoming identification spectrum (Fig. 1, left), a specific ion is chosen using an elliptical cut where the axes of the ellipse correspond to 2σ values of the charge and A/Q distributions. In this case, the isotope having $Z = 50$ and $A/Q = 2.48$ corresponding to ^{124}Sn is selected.

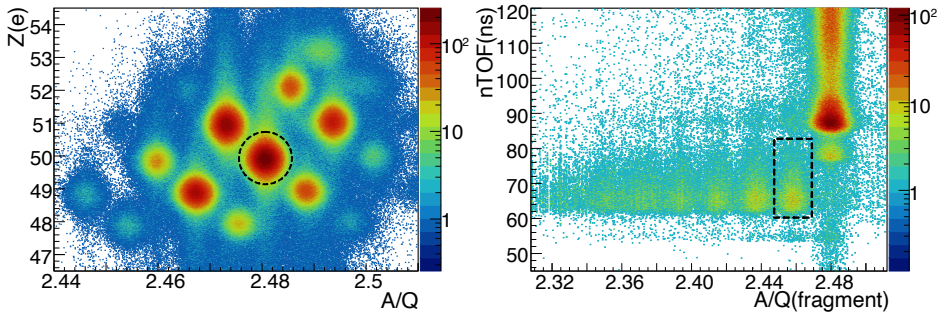

Fig. 1. Incoming ID for ^{124}Sn setting at 904 MeV/u (left) and correlation between neutron ToF (nToF) and A/Q of detected tin fragments for incoming ^{124}Sn (right).

The reaction channel of interest is selected in the 2D histogram showing correlations between the time of flight (ToF) measured in the neutron detector and the A/Q of the fragment (Fig. 1, right). For the current analysis, the fragment velocity is approximated with the incoming beam velocity. The one-neutron ($1n$) channel corresponds to events inside the rectangle centered at 2.46 in A/Q (^{123}Sn). The used cut encloses a 2σ range from the mean in A/Q and a 60–83 ns ToF range. At $A/Q = 2.48$ (^{124}Sn), one can notice the absence of coincidences in the neutron ToF region, while the structures above ≈ 76 ns are well-separated background reactions from beam particles at the end of the fragment arm and the beam dump where secondaries introduce a signal in the neutron detector. In the right panel of Fig. 1, higher

neutron multiplicity events associated with $A/Q < 2.46$ can be noticed. To extract their contribution to the cross section, the multi-neutron analysis will have to be performed including simulations from which reconstruction efficiencies can be obtained. The Coulomb excitation cross section in the lead target is calculated according to

$$\sigma_{\mathrm{C}} = \frac{M(\mathrm{Pb})}{d(\mathrm{Pb})N_{\mathrm{A}}}[p_{\mathrm{Pb}} - p_{\mathrm{empty}}] - \alpha(\mathrm{Pb},\mathrm{C})\frac{M(\mathrm{C})}{d(\mathrm{C})N_{\mathrm{A}}}[p_{\mathrm{C}} - p_{\mathrm{empty}}]\,, \qquad (1)$$

where p_{i} denotes the reaction probability which is determined as the ratio of events from a certain target and the total number of incoming projectiles. To account for secondary reactions occurring in the target or elsewhere in the detector setup and tracking efficiency, an approximation was made where the number of incoming projectiles was substituted with the number of unreacted projectiles at the end of the setup ($\approx 35\%$ difference) [4]. The molar mass of the target material and the thickness of the target are denoted with M and d, respectively, while N_{A} is the Avogadro constant. For the background subtraction, the above-mentioned empty target is used, while the carbon target serves the purpose of subtracting nuclear contribution to σ_{C}. The latter assumes that most interactions with carbon will be of nuclear origin due to its small atomic number. The cross section determined with the carbon target is scaled by the factor α, taking into account the size difference between carbon and lead nuclei [11]

$$\alpha = \frac{1 + aA_{\mathrm{Pb}}^{1/3}}{1 + aA_{\mathrm{C}}^{1/3}}\,, \qquad a = 0.14 \pm 0.01\,. \qquad (2)$$

The efficiency and acceptance of the neutron detector were obtained from Geant4 simulations. The $1n$ detection efficiency at 904 MeV is obtained as $\approx 80\%$. The acceptance is calculated as a function of the neutron kinetic energy. Up to ≈ 5 MeV neutron kinetic energy (in the fragment rest frame), the acceptance is 100%, above, it starts to decrease and at 35 MeV, it falls below 20%. An additional cut was applied at 15 MeV corresponding to the adiabatic cutoff energy (for details, see Ref. [4]) from which one-neutron separation energy was subtracted. Although this was evaluated as a good starting estimate, refined calculations of statistical decay should give a more accurate limit. Both statistical and systematic errors (stemming from efficiency and acceptance uncertainties) are taken into account. The contamination remaining after the cuts applied on outgoing fragments and neutrons is yet to be examined in more detail. The value of preliminary $1n$ cross section is determined as $\sigma_{\mathrm{C}}(1n) = (1130 \pm 77)$ mb.

In ^{124}Sn, the one-neutron separation energy lies around 8.5 MeV, while the two-neutron separation energy is found at approximately 14.4 MeV. The GDR is located near 15 MeV, hence $1n$ decay is expected to be the largest contribution to the σ_{C} among other neutron decay channels since the phase space for possible decays is the largest (which is also confirmed in Ref. [4]).

From the theoretical side, calculations of σ_{C} will be performed following the virtual photon formalism [1] as well as the coupled channel method [12] using the input from various relativistic and non-relativistic energy density functionals. The comparison with theoretical calculations which will include an examination of other multipoles, as well as a more detailed subtraction method of the nuclear contribution to the measured cross section, will be made once other neutron decay channels have been analyzed.

This work has been supported in part by the Croatian Science Foundation under project No. IP-2018-01-1257, and in part by the Center of Excellence for Advanced Materials and Sensing Devices, grant No. KK. 01.1.1.01.0001.

REFERENCES

[1] C.A. Bertulani, G. Baur, *Phys. Rep.* **163**, 299 (1988).
[2] P. Adrich *et al.*, *Phys. Rev. Lett.* **95**, 132501 (2005).
[3] X. Roca-Maza, N. Paar, *Prog. Part. Nucl. Phys.* **101**, 96 (2018).
[4] A. Horvat, Ph.D. Thesis, TU Darmstadt, 2019.
[5] D.M. Rossi *et al.*, *Phys. Rev. Lett.* **111**, 242503 (2013).
[6] H. Geissel *et al.*, *Annu. Rev. Nucl. Part. Sci.* **45**, 163 (1995).
[7] H. Alvarez-Pol *et al.*, *Nucl. Instrum. Methods Phys. Res. A* **767**, 453 (2014).
[8] M. Heil *et al.*, *Eur. Phys. J. A* **58**, 248 (2022).
[9] K. Boretzky *et al.*, *Nucl. Instrum. Methods Phys. Res. A* **1014**, 165701 (2021).
[10] V. Panin *et al.*, *Phys. Lett. B* **797**, 134802 (2019).
[11] K. Boretzky, Ph.D. Thesis, Universität Frankfurt am Main, 1995.
[12] C.A. Bertulani *et al.*, *Phys. Rev. C* **53**, 334 (1996).